



King Saud University  
Arabian Journal of Chemistry

[www.ksu.edu.sa](http://www.ksu.edu.sa)  
[www.sciencedirect.com](http://www.sciencedirect.com)



## ORIGINAL ARTICLE

# Adsorption of ibuprofen from aqueous solution on chemically surface-modified activated carbon cloths

Hanen Guedidi <sup>a,b</sup>, Laurence Reinert <sup>a</sup>, Yasushi Soneda <sup>c</sup>, Nizar Bellakhal <sup>b</sup>,  
Laurent Duclaux <sup>a,\*</sup>

<sup>a</sup> Univ. Savoie, LCME, F-73000 Chambéry, France

<sup>b</sup> Laboratoire de Chimie Analytique et Electrochimie, Université de Tunis, 2092 Manar II, Tunisia

<sup>c</sup> National Institute of Advanced Industrial Science and Technology, Energy Technology Research Institute, 16-1 Onogawa, Tsukuba, Ibaraki 305-8569, Japan

Received 17 September 2013; accepted 13 March 2014

## KEYWORDS

Activated carbon cloth;  
Ibuprofen;  
Porosity;  
Thermodynamic parameters;  
Kinetics

**Abstract** This study aims to investigate the performance of an activated carbon cloth for adsorption of ibuprofen. The cloth was oxidized by a NaOCl solution ( $0.13 \text{ mol L}^{-1}$ ) or thermally treated under  $\text{N}_2$  ( $700 \text{ }^\circ\text{C}$  for 1 hour). The raw and modified cloths were characterized by  $\text{N}_2$  adsorption–desorption measurement at 77 K,  $\text{CO}_2$  adsorption at 273 K, Boehm titrations,  $\text{pH}_{\text{PZC}}$  measurements, X-ray Photoelectron Spectroscopy analysis, and by infrared spectroscopy. The NaOCl treatment increases the acidic sites, mostly creating phenolic and carboxylic groups and decreases both the specific surface area and slightly the micropore volume. However, the thermal treatment at  $700 \text{ }^\circ\text{C}$  under  $\text{N}_2$  induced a slight increase in the BET specific surface area and yielded to the only increase in the carbonyl group content. Ibuprofen adsorption studies of kinetics and isotherms were carried out at  $\text{pH} = 3$  and 7. The adsorption properties were correlated to the cloth porous textures, surface chemistry and pH conditions. The isotherms of adsorption were better reproduced by Langmuir–Freundlich models at 298, 313 and 328 K. The adsorption of ibuprofen on the studied activated carbon cloths at  $\text{pH} 3$  was an endothermic process. The pore size distributions of all studied ibuprofen-loaded fabrics were determined by DFT method to investigate the accessible porosity of the adsorbate. Both treatments do not influence the kind of micropores where the adsorption of ibuprofen occurred.

© 2014 King Saud University. Production and hosting by Elsevier B.V. All rights reserved.

## 1. Introduction

Activated carbons are traditionally in the form of powder or granule, but in the last few decades activated carbon fibers were developed. They have received considerable attention as potential adsorbents for water treatment applications in the form of felt or cloth. Despite of their higher cost, they have several technological advantages in comparison with traditional forms, including faster pore diffusion and adsorption kinetics, a high

\* Corresponding author. Tel./fax: +33 479758805.  
E-mail address: [laurent.duclaux@univ-savoie.fr](mailto:laurent.duclaux@univ-savoie.fr) (L. Duclaux).

Peer review under responsibility of King Saud University.



Production and hosting by Elsevier

specific surface area, well developed microporous structure and they can be easily handled (Ayranci and Duman, 2006).

Activated carbon fibers were widely used for removal of several pollutants such as dyes (Jiang et al., 2013), heavy metals (Afkhami et al., 2007; Faur-Brasquet et al., 2002) or pesticides (Ania and Beguin, 2007; Ayranci and Hoda, 2005), whereas, very few studies concerned the removal of pharmaceutical products by this form of activated carbon (Mestre et al., 2011). Due to its widespread applications as an anti-inflammatory and antipyretic drug, ibuprofen is frequently detected in the wastewater treatment plants among several other pharmaceutical molecules (Verlicchi et al., 2010). Very recently, Khalaf et al. compared the adsorption of ibuprofen between a clay micelle complex and an activated carbon charcoal and demonstrated that both adsorbents had comparable efficiencies for the removal of this pharmaceutical molecule (Khalaf et al., 2013). Some other activated carbons of different origins and physico-chemical properties were recently studied for the removal of ibuprofen from aqueous solutions (Mestre et al., 2007, 2009; Dubey et al., 2010; Baccar et al., 2012).

Surface modifications of activated carbon are an attractive route to obtain materials with different textural properties and various surface chemistries. Among the oxidative modification treatments such as air oxidation, electrochemical oxidation, plasma treatment, and Fenton treatment; treatment with oxidizing agents such as  $\text{HNO}_3$ ,  $\text{H}_2\text{O}_2$ ,  $(\text{NH}_4)_2\text{S}_2\text{O}_8$ , and  $\text{NaOCl}$  is known to generate an increase in oxygenated surface functional groups (Moreno-Castilla et al., 2000; Pradhan and Sande, 1999).

Several studies were devoted to the carbon materials' oxidation by  $\text{NaOCl}$  (Su et al., 2010; Perrard et al., 2012). For example Su et al. (2010) have reported that the physico-chemical properties of carbon nanotubes and their ability for removing organic pollutants were greatly improved after the oxidation by  $\text{NaOCl}$ . More recently, Perrard et al. (2012) distinguished the stages in the  $\text{NaOCl}$  oxidation kinetics at ambient temperature of an activated carbon cloth: leading after a deep attack to the fabric dismantling and the fibers' breakage. Besides, surface modification of activated carbons by thermal treatment under inert atmosphere is known to lead to higher basic materials (Papirer et al., 1987; Carrott et al., 2001; Valente Nabais et al., 2004). Pereira et al. (2003) have found that among several modifications, the thermal treatment of a commercial activated carbon was the best for adsorption of several cationic and anionic dyes. In our previous study (Guedidi et al., 2013), we have also found that the thermal treatment under  $\text{N}_2$  of a granular activated carbon could produce basic sites increasing the uptake of ibuprofen.

The aim of the present work was to study the influence of the modification of an activated carbon cloth on the adsorption properties of ibuprofen. In order to obtain materials with different surface chemistry and textural properties, the activated carbon cloth has undergone two different treatments: oxidation by  $\text{NaOCl}$  and thermal treatment under nitrogen. The textural structures of the activated carbon cloths were characterized. The surface oxygen containing groups were analyzed by XPS (X-ray Photoelectron Spectroscopy analysis), ATR infrared Fourier transform spectroscopy (ATR-FTIR) and Boehm titration separately. We have tentatively evaluated the role of the modification of surface chemistry on the interaction between the ibuprofen molecule and the activated carbons' surface through the investigation of kinetics pH

dependence and of isotherms at various temperatures. We have also studied the porosity accessible to this molecule before and after each treatment.

## 2. Experimental

### 2.1. Materials

2-[4-(2-Methylpropyl) phenyl]propanoic acid, also named ibuprofen (IBP), was purchased from Sigma-Aldrich (>98% purity). The atomic positions of IBP were determined by molecular modelization using chemsketch 3D viewer. The dimensions of the molecule included in a parallelepiped ( $1.36$  (length)  $\times$   $0.74$  (width)  $\times$   $0.52$  (thickness)  $\text{nm}^3$ ) were obtained by adding the Van der Waals radius value (0.1 nm) to the Hydrogen atoms at extreme positions. These dimensions are in agreement with those found by Azaïs et al. (2006).

The raw activated carbon cloth (900-20) referred to C0 was provided by Kuraray Chemical Co. Ltd. (Japan). Prior to modification, it was stirred in 0.1  $\text{mol L}^{-1}$  hydrochloric acid solution for 24 h to remove metal salt impurities. After filtration, it was rinsed with distilled water ( $\sim 200$  mL per g) until reaching a constant pH of the filtrate and dried at 383 K for 24 h. The dried sample was further modified by (i) bleaching or (ii) thermal treatment, and (iii) further ibuprofen loaded as following:

- (i) 1 g of C0 was stirred in 200 mL of a 0.13  $\text{mol L}^{-1}$   $\text{NaOCl}$  solution at room temperature for 24 h. After filtration, washing and drying, the recovered bleached sample was named CNaOCl.
- (ii) About 2.5 g of C0 was heated under a nitrogen flow in a tubular furnace at 973 K (ramp of 10  $\text{K min}^{-1}$ ) and maintained at this temperature for 1 h. Sample was kept under inert atmosphere until cooling to room temperature. Recovered cooled sample was named C700N2.
- (iii) To investigate the porosity accessible to ibuprofen, 200 mg of each sample (C0, CNaOCl and C700N2) was saturated by ibuprofen (1 L, 100  $\text{mg L}^{-1}$ ) at pH 7, at maximum uptake for 5 days and compared to the raw fabric activated carbon.

### 2.2. Textural and chemical characterization of activated carbons

The porosity of the activated carbon cloths was characterized by  $\text{N}_2$  adsorption-desorption at 77 K and  $\text{CO}_2$  adsorption at 273 K using an automatic sorptometer (ASAP 2020, Micromeritics). Prior to measurements, samples have been degassed for 12 h at 523 K under vacuum.

The  $\text{N}_2$ -isotherms were used to calculate the specific surface area using the Brunauer-Emmett-Teller (BET) equation, assuming the area of the nitrogen molecule to be 0.162  $\text{nm}^2$ . As negative unrealistic C factors were obtained by applying the BET model in the relative pressure range from 0.05 to 0.3, the BET specific surface areas were preferentially computed in the relative pressure range of 0.01-0.05, as for microporous materials (Kaneko and Ishii, 1992).

The total pore volume was estimated as the liquid volume of  $\text{N}_2$  adsorbed at a relative pressure of 0.995. Pore size distributions (PSD) of the activated carbon samples were determined by using NLDFT (non local density functional

theory) models applied on the adsorption isotherms of N<sub>2</sub> at 77 K. Additionally, the distribution of pores smaller than 0.7 nm (narrow micropores or ultramicropores) was evaluated from CO<sub>2</sub> adsorption isotherms at 273 K. For that, infinite slit pore model was assumed for CO<sub>2</sub> adsorption (pores diameter lower than 1.1 nm), while finite slit pore model was used for N<sub>2</sub> adsorption simulations (Jagiello and Olivier, 2009). N<sub>2</sub> adsorption data at  $P/P_0 < 0.01$  were obtained using incremental fixed doses of  $\sim 10 \text{ cm}^3 \text{ g}^{-1}$  (STP), setting the equilibration interval at 300 s. CO<sub>2</sub> adsorption data were obtained at  $P/P_0$  ranging from  $4 \times 10^{-4}$  to  $3.5 \times 10^{-2}$ , using 45 s equilibration interval (Jagiello and Thommes, 2004).

The DFT pore size distributions of the IBP loaded activated carbon cloths (at pH 7) were studied in the same condition as that of the raw cloth but after degassing at 323 K for 4 days under secondary vacuum to avoid the decomposition of ibuprofen of which melting point is equal to 348–350 K (Lerdkanchanaporn and Dollimore, 2000).

The pH of each activated carbon cloth (0.5 g) was measured in a distilled water suspension (12.5 mL) after heating at 90 °C and then cooling to room temperature (Reffas et al., 2010).

The  $\text{pH}_{\text{PZC}}$ , i.e. the pH of the solution when the net surface charge equals zero, was determined by the so-called pH drift method (Franz et al., 2000). Mixtures of 0.15 g of activated carbon cloths and 50 mL of deoxygenized 0.01 mol L<sup>-1</sup> NaCl solutions of initial pH values varying from 2 to 12 were stirred for 48 h under N<sub>2</sub> in order to avoid the formation of dissolved CO<sub>2</sub>. The final pH was measured and plotted against the initial pH. The  $\text{pH}_{\text{PZC}}$  was equal to the value for which  $\text{pH}(\text{final}) = \text{pH}(\text{initial})$ .

Boehm titrations quantify the basic and oxygenated acid surface groups on activated carbons (Boehm, 2002). Surface functional groups such as carboxyl (R–COOH), lactone (R–OCO), phenol (Ar–OH), carbonyl or quinone (RR'C=O) and basic groups were determined using different reactants, assuming that NaOC<sub>2</sub>H<sub>5</sub> reacted with all groups; NaOH did not react with RR'C=O groups; Na<sub>2</sub>CO<sub>3</sub> did not react with RR'C=O nor R–OH groups and that NaHCO<sub>3</sub> only reacted with R–COOH groups. About 0.15 g of each carbon sample was mixed in a closed Erlenmeyer with 50 mL of a 0.1 mol L<sup>-1</sup> aqueous reactant solution (NaOH, Na<sub>2</sub>CO<sub>3</sub> or NaHCO<sub>3</sub>). In the case of NaOC<sub>2</sub>H<sub>5</sub>, only 0.1 g of carbon sample was added to 50 mL of 0.01 mol L<sup>-1</sup> solutions which were prepared in absolute ethanol. The mixtures were stirred for 24 h at constant speed (650 rpm) and room temperature and then filtered off. Back-titrations of the filtrate (10 mL) were then achieved with standard HCl (0.01 mol L<sup>-1</sup>) to determine the oxygenated group contents. Basic group contents were also determined by back titration of the filtrate with NaOH (0.01 mol L<sup>-1</sup>) after stirring the activated carbon (0.15 g) in HCl (50 mL, 0.01 mol L<sup>-1</sup>) for 24 h.

The surface of activated carbons was characterized by ATR-FTIR using a Thermo Scientific Nicolet iS10 spectrometer equipped with a germanium crystal. A DTGS KBr detector was used for detection and the incident angle of the beam was 45°. All spectra were collected in the infrared region [500–4000 cm<sup>-1</sup>] with a spectral resolution of 4 cm<sup>-1</sup>. 64 scans were accumulated for each analysis.

X-ray photoelectron spectroscopy (XPS) measurements were performed using an ESCALAB 250 spectrometer (Thermo Fisher Scientific) at monochromatic Al-K $\alpha$  anode X-ray radiation, on a 150 × 800  $\mu\text{m}^2$  analysis region, under

$2 \times 10^{-9}$  mbar vacuum. The high-resolution scans (0.1 eV) were obtained over the 280.1–299.9 eV (C1s) and 523.1–539.9 eV (O1s) energy ranges with a pass energy of 20 eV. After baseline subtraction, the curve fitting was performed assuming a mixed Gaussian–Lorentzian peak shape (the ratio of Gaussian to Lorentzian form was equal to 0.3). The carbon 1s electron binding energy corresponding to graphitic carbon was referenced at 284.6 eV for the calibration (Xie and Sherwood, 1990).

### 2.3. Adsorption experiments: Isotherms and kinetics

All the IBP solutions were prepared from UHQ water (Ultra High Quality, 18.2 M $\Omega$  purity) containing 10 vol.% of methanol (99.9%) in order to increase the IBP solubility.

The kinetics were studied at 298 K at pH 3 and 7. The initial pHs of IBP solutions were adjusted at pH 3 and 7 by adding either 0.1 mol L<sup>-1</sup> HCl or NaOH. Suspensions of 10 mg of the activated carbon cloth in 100 mL of 100 ppm IBP solution were stirred at 250 rpm and then filtered at different times between 5 min and 7 days.

Adsorption isotherms of IBP on the different activated carbon cloths were performed at pH 3 at constant temperatures of 298, 313 and 328 K. 10 mg of activated carbon cloths was introduced in IBP solutions (100 mL) of varying initial concentrations (5–100 mg L<sup>-1</sup>). Suspensions have been stirred for 5 days in a thermostatically controlled orbital shaker (New Brunswick Scientific, Innova 40, and stirring speed of 250 rpm) to reach equilibrium and then filtered. The initial and residual IBP concentrations were measured by high performance liquid chromatography (HPLC) using a Waters chromatograph equipped with a high pressure pump (Waters 515), a photodiode array detector (Waters 996) and a Sunfire C18 column (5  $\mu\text{m}$ , 4.6 × 250 mm). A methanol/ultrapure water solution (80/20, v/v), containing 0.1 vol.% of concentrated phosphoric acid (95 wt.%) in isocratic mode at a flow rate of 1 mL min<sup>-1</sup> was used as mobile phase. Detection was operated at 220 nm.

The equilibrium IBP uptake  $Q_{\text{ads}}$  (mg g<sup>-1</sup>) was calculated from equation:

$$Q_{\text{ads}} = \frac{(C_e - C_i) \cdot V}{m}$$

where  $V$  is the solution volume (L),  $C_i$  is the initial IBP concentration (mg L<sup>-1</sup>),  $C_e$  is the equilibrium IBP concentration (mg L<sup>-1</sup>) and  $m$  is the mass of the dry activated carbon cloth (g).

## 3. Results and discussion

### 3.1. Characterization of activated carbons

#### 3.1.1. Surface chemistry

The results of Boehm titrations (Table 1) indicated that C0 was mainly acidic: the amount of oxygenated groups ( $\sim 0.84 \text{ meq g}^{-1}$ ) was about twice the one of basic groups ( $\sim 0.43 \text{ meq g}^{-1}$ ). This was confirmed by the slightly acidic pH measured value (6.05). The higher value of  $\text{pH}_{\text{PZC}}$  (8.40) might be assigned to the presence of high contents of carbonyl groups ( $\text{p}K_{\text{a}}\text{-carbonyl} \sim 16\text{--}20$ ).

Thermal treatment under N<sub>2</sub> removed virtually the totality of the carboxylic and lactonic groups and significantly

**Table 1** Surface groups (in meq g<sup>-1</sup>) obtained from “Boehm” titrations, pH and pH<sub>PZC</sub> values of raw and modified activated carbon cloths.

Activated carbon sample	C0	CNaOCl	C700N <sub>2</sub>
Carboxylic groups	0.04	0.56	0
Lactonic groups	0.12	0.42	0
Phenolic groups	0.02	0.19	0.03
Carbonyl groups	0.66	0.51	1.36
Total oxygenated groups	0.84	1.68	1.39
Total basic groups	0.43	0.28	0.62
pH	6.05	5.59	7.52
pH <sub>PZC</sub>	8.40	6.54	7.80

increased the number of carbonyl group compared to C0 (Table 1). The substrate has become slightly basic (pH = 7.52 and pH<sub>PZC</sub> = 7.80) due to the high reactivity of the newly treated surface with regards to dioxygen upon re-exposure in air (Menéndez et al., 1996). As a consequence, new oxygenated groups (mainly carbonyl groups) were generated after aging of C700N<sub>2</sub>.

The treatment of the activated carbon cloth with NaOCl has increased the amount of total oxygenated groups (from 0.84 to 1.68 meq g<sup>-1</sup>) and led to a decrease in the number of basic sites (Table 1). As expected, this oxidative treatment increased the carboxylic group content, created lactones and phenols but slightly decreased the number of carbonyl groups. As a consequence, the measured pH<sub>PZC</sub> and pH values for CNaOCl were the lowest.

The evolution of the surface chemistry induced by both treatments was also characterized by XPS. The C1s spectra (not shown) were deconvoluted into four peaks (Table 2) attributed to carbon present in: graphitic layers (peak I), phenolic or alcohol groups (peak II), carbonyl or quinone groups (peak III), and carboxylic or ester or lactonic groups (peak IV). The three peaks issued from the deconvolution of the O1s spectra (Table 2) were attributed to C=O groups (peak A), C–O groups (peak B) and to chemisorbed oxygen (peak C).

For all samples, the peak of highest intensity was attributed to graphitic carbon (~284.6 eV). The relative intensity of this main signal decreased for both treated samples as oxygenated functional groups were formed. Indeed, the total percentage of atomic oxygen measured increased from 4.71% for C0 to 12.98 at.% and 27.40 at.% for samples C700N<sub>2</sub> and CNaOCl, respectively. An increase in the intensities of the signals attrib-

uted to carbon atoms linked to oxygen ones was also observed for both treated samples compared to sample C0 (peaks labeled II, III and IV).

For sample CNaOCl, the increase in oxygen groups observed by XPS (Table 2) is mainly due to the formation of additional phenolic and carboxylic groups, in agreement with the Boehm titrations (Table 1). Similarly, Perrard et al. (2012) reported after oxidation of an ex-cellulose activated carbon cloth by NaOCl (0.53 mol L<sup>-1</sup>, 90 min), an increase in the carboxylic and phenolic group content was observed by XPS, but later phenolic groups were oxidized up to lactonic groups. Cagnon et al. (2005) reported an increase in carboxylic and carbonyl groups observed by XPS, after bleaching of an activated carbon. Indeed, in one of our previous studies (Guedidi et al., 2013), we also found that a commercial granular activated carbon oxidized by NaOCl presented a slight increase in carbonyl and carboxylic contents compared to the raw activated carbon.

Moreover, the XPS O–C contribution has increased for both modified cloths and especially for CNaOCl (from 1.66 to 19.85 at.%), which is in agreement with Boehm titrations. Furthermore, the chemisorbed oxygen increases after oxidation by NaOCl from 1.37 to 2.71 at.% (Table 2). It can be explained by the presence of water attributed to the increase in the surface hydrophilicity for CNaOCl.

For C700N<sub>2</sub>, the oxygen increase observed by XPS (Table 2) originates from the formation of C=O and O–C=O bonds. The increase in carbonyl (C=O) is in agreement with Boehm titration. The carboxylic groups were found absent by Boehm titrations, thus the O–C=O bonds were possibly ester or lactonic groups. Virtually, most of the studies (Rong et al., 2003; Swiatkowski et al., 2004) on the thermal treatment of activated carbon under inert atmosphere reported that all oxygen containing functional groups were removed during this treatment. But, the work of Menéndez et al., (1996) showed the temporary efficiency of such treatment for removing the oxygen containing surface groups, as reactive surface sites are known to be generated. As the resultant surface is very active, it can react with oxygen present in air, giving new surface oxide such as carbonyls. These groups have a basic character, conferring basic properties to the activated carbon.

The infrared ATR spectra of C0 and C700N<sub>2</sub> are very similar (Fig. 1 a and b) and show a broad band between 1000 and 1250 cm<sup>-1</sup> assigned to C–O stretching in acids, alcohols, phenols, ether and esters (Park et al., 1999). These observations suggest that these groups remained present on the activated

**Table 2** Atomic percentages of carbon (C1s) and oxygen (O1s) obtained by XPS analysis of raw and modified activated carbon cloths.

Peak	Binding energy (eV)	Signal attribution E(eV)	C0	CNaOCl	C700N <sub>2</sub>
I	284.6	C–C	74.89	40.82	57.34
II	285.09–285.24	C–O	13.57	17.98	12.60
III	286.21–286.35	C=O	6.83	7.29	8.99
IV	287.93–288.36	O–C=O	0	6.50	8.10
A	531.21–531.90	O=C	1.68	4.84	5.16
B	532.96–533.33	O–C	1.66	19.85	6.36
C	535.01–535.75	Chemisorbed O	1.37	2.71	1.46
Total atomic O			4.71	27.40	12.98

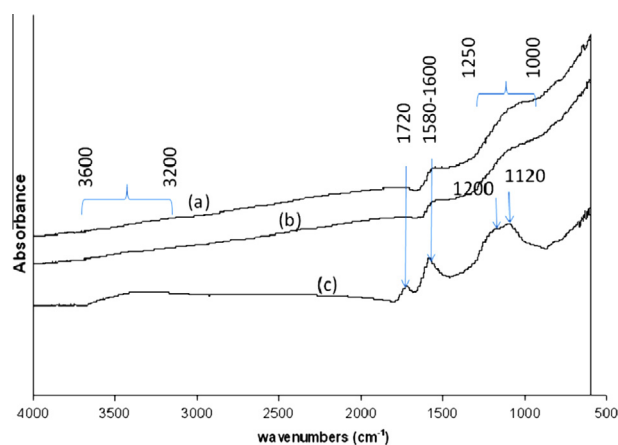


**Figure 1** FTIR spectra of (a) C700N2; (b) C0 and (c) CNaOCl.

carbon cloth surface even after treatment at 973 K under  $N_2$ , in agreement with the results obtained by Boehm titrations and XPS (similar content of phenolic and lactonic groups before and after thermal treatment under  $N_2$ ).

In CNaOCl ATR spectrum (Fig. 1c), the intensity of this band was increased exhibiting two maxima at 1120 and 1200  $cm^{-1}$  assigned to C–O stretching in ester or other groups due to bleaching (Tables 1 and 2).

Moreover, after the bleaching treatment, a new broad band appeared in the 3200–3600  $cm^{-1}$  range due to the O–H stretching vibration of phenolic groups and chemisorbed water (Biniak et al., 1997). The peak centered at 1720  $cm^{-1}$ , only observed on the spectrum of CNaOCl, is assigned to the C=O stretching vibration of ketone, ester and/or aromatic carboxylic groups (Perrard et al., 2012). All spectra present a peak at 1580–1600  $cm^{-1}$  assigned to C=C stretching modes of aromatic rings or to C=O groups stretching vibrations conjugated with aromatic rings (Sabio et al., 2004). This peak (at 1600  $cm^{-1}$ ) was also noticeably increased after NaOCl treatment (Fig. 1c), possibly after the formation of carboxylic, lactonic and quinone groups (Table 1). As conjugation moves absorptions to lower wavenumbers, this peak is shifted to 1580  $cm^{-1}$  for C700N2 and C0 (Domingo-Garcia et al., 2000).

### 3.1.2. Porosity characterization

Fig. 2a and b shows the nitrogen adsorption–desorption isotherms of raw and modified fabrics. All the isotherms belong to the type I, typical of microporous materials, according to the IUPAC classification. They present a sharp knee in the low relative pressure region and a very low slope in the multi-layer range (at higher pressure), indicating the absence of significant mesoporosity. Indeed, insignificant mesopore volumes were measured for the three samples (Table 3). The isotherm profiles are characteristic of narrow micropore samples. After NaOCl treatment, the  $N_2$  uptake at high relative pressure was significantly reduced, explaining the decrease of the BET specific surface area to 1690  $m^2 g^{-1}$  in comparison with the C0 one (1910  $m^2 g^{-1}$ ). The decrease in the BET specific surface area is related to the decrease in the micropore volume which might be filled by the surface functional groups formed through NaOCl oxidation. This treatment yields also to the supermicropore slight decrease from 0.32 to 0.26  $cm^3 g^{-1}$ , possibly explained by the collapse of some pore walls during

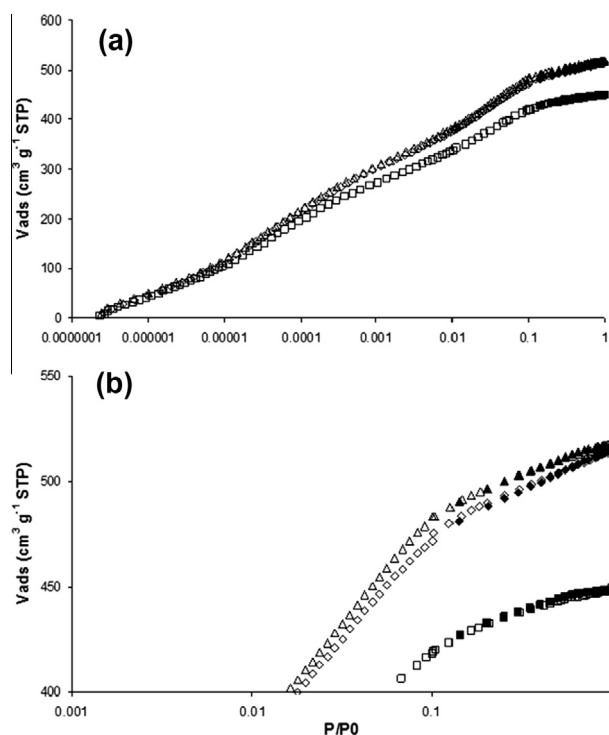


**Figure 2** (a)  $N_2$  adsorption–desorption isotherms at 77 K of the pristine C0 (◇: adsorption, ♦: desorption), CNaOCl (□: adsorption, ■: desorption) and C700N2 (△: adsorption, ▲: desorption); (b) Zoom of  $N_2$  adsorption–desorption isotherms of C0, CNaOCl and C700N2.

oxidation. Table 3 shows for C700N2 a very slight increases both in BET specific surface area (1946  $m^2 g^{-1}$ ) and in micropore volumes, which might result from the thermal decomposition of the oxygenated surface groups that were either inside the micropores or blocking micropore entrances (Pereira et al., 2003). However this increase is not significant as the measured ultramicropore and supermicropore volumes remain constant after thermal treatment.

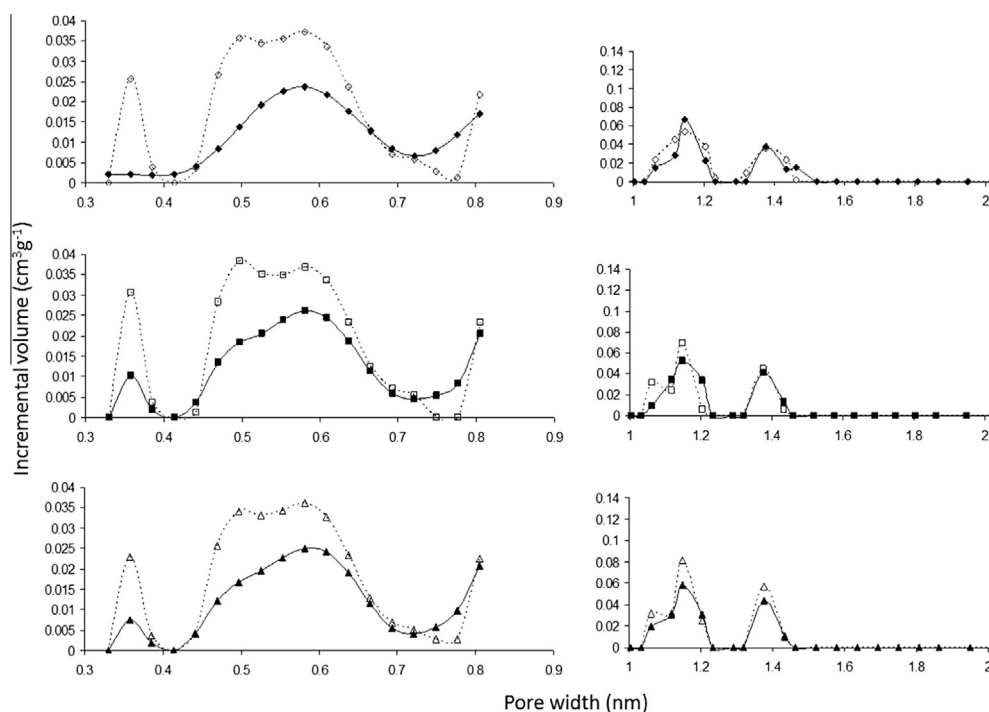
The study of the PSD of the IBP-loaded samples and the initial adsorbents brought out that this molecule might mainly adsorb in the ultramicropores and slightly in the supermicropore (Fig. 3) as previously reported by Guedidi et al. (2013). The ultramicropore volumes clearly decreased after IBP adsorption while the supermicropore volume slightly decreased (Table 3). From PSDs obtained from  $CO_2$  isotherms, it can be concluded that whatever the fabric sample: C0, C700N2, or CNaOCl, the adsorption of IBP might occur mainly in the ultramicropores of diameter lower than 0.7 nm (Fig. 3).

However, a rough calculation shows that IBP can only access to slit-pores of inter-wall spacing higher than 0.7 nm by taking into account the thickness of the molecule (0.5 nm) and the atomic radius of the adsorbent on both sides of the pore walls (almost 0.1 nm). This means that theoretically IBP should not be accommodated in the ultramicropores. Possibly, the IBP molecule could access the larger ultramicropores after a modification of its geometry.

Table 4 shows also the IBP occupied volumes in ultramicropores and supermicropores calculated from the difference between porous volume of the initial samples and the IBP

**Table 3** Textural properties obtained by N<sub>2</sub> adsorption/desorption and CO<sub>2</sub> adsorption studies.

Sample	C0	CNaOCl	C700N2	C0(IBP)	CNaOCl(IBP)	C700N2(IBP)
S <sub>BET</sub> (m <sup>2</sup> g <sup>-1</sup> )	1910	1690	1946	1244	1161	1240
Total pore volume(cm <sup>3</sup> g <sup>-1</sup> )	0.79	0.69	0.80	0.51	0.48	0.51
Micropore volume <sup>a</sup> (cm <sup>3</sup> g <sup>-1</sup> )	0.75	0.65	0.76	0.47	0.44	0.48
Mesopore volume <sup>a</sup> (cm <sup>3</sup> g <sup>-1</sup> )	0.04	0.04	0.04	0.04	0.04	0.03
Ultramicropore volume <sup>b</sup> (cm <sup>3</sup> g <sup>-1</sup> )	0.31	0.31	0.30	0.12	0.14	0.14
Supermicropore volume <sup>a</sup> (cm <sup>3</sup> g <sup>-1</sup> )	0.32	0.26	0.32	0.25	0.22	0.24

<sup>a</sup> From N<sub>2</sub> DFT.<sup>b</sup> From CO<sub>2</sub> DFT.**Figure 3** NLDFT pore size distributions either for narrow micropores (<0.7 nm) from CO<sub>2</sub> adsorption isotherms at 273 K, or for supermicropores (1 nm < Ø < 2 nm) from N<sub>2</sub> adsorption isotherms at 77 K: of C0 (◇) and 134.7 mg g<sup>-1</sup> IBP loaded C0 (◆), of CNaOCl (□) and 119 mg g<sup>-1</sup> IBP loaded CNaOCl (■) and of C700N2 (Δ) and 127.05 mg g<sup>-1</sup> IBP loaded C700N2 (▲).**Table 4** Comparison of the occupied ultramicropore volumes (from DFT PSD) and the IBP occupied volume calculated from the uptake.

	Vultramicropore occupied by IBP (cm <sup>3</sup> g <sup>-1</sup> ) <sup>a</sup>	Vsupermicropore occupied by IBP (cm <sup>3</sup> g <sup>-1</sup> ) <sup>a</sup>	IBP volume uptake <sup>b</sup> (cm <sup>3</sup> g <sup>-1</sup> )
C0	0.19	0.07	0.20
CNaOCl	0.17	0.04	0.18
C700N2	0.16	0.08	0.19

<sup>a</sup> Calculated from the PSD volume differences.<sup>b</sup> Calculated from the IBP measured uptake and dimension size.

loaded samples (ultramicropore and supermicropore volumes were obtained from PSD DFT models from CO<sub>2</sub> and N<sub>2</sub> isotherms, respectively). These volumes were compared to the volume uptake obtained from the IBP measured adsorption uptake taking into account its calculated volume (0.52 nm<sup>3</sup>). The whole IBP occupied micropore volumes (ultra-

micropore + supermicropore) calculated for all carbons (Table 4) were higher than the IBP volumic uptake suggesting the IBP pore space blocking leading to the formation of sealed inaccessible porosities particularly in ultramicropores. This also suggests the IBP accommodation both in larger ultramicropores and supermicropores.

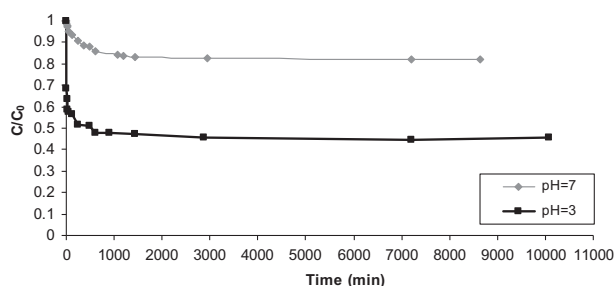


**Figure 4** Ibuprofen adsorption kinetics onto C0 cloth at 298 K at pH 3 and 7 ([IBP] = 100 mg L<sup>-1</sup>,  $m_{\text{adsorbent}} = 10$  mg,  $V_{\text{IBP}} = 100$  mL, stirring speed = 250 rpm).

### 3.2. Ibuprofen adsorption kinetics and pH effect

The  $pK_a$  of ibuprofen is equal to 4.91 (Lindqvist et al., 2005). The effect of the initial pH on the IBP adsorption kinetics onto the C0 cloth was studied at  $\text{pH} \sim pK_a - 2$  and  $\text{pH} \sim pK_a + 2$  (i.e.  $\text{pH} = 3$  and 7) at 298 K, where IBP was either molecular, or negatively charged. The plot of  $C/C_0$  vs time (Fig. 4) shows that the adsorption kinetic is faster at pH 3 than at pH 7. Indeed, the equilibrium adsorption times, corresponding to the appearance of the plateaus on both curves, are of about 600 min and 1440 min at pH 3 and 7, respectively.

Moreover, Fig. 4 shows that the IBP uptake increases when the pH decreases. As the C0 fabric surface is positively charged and the molecule is neutral at pH 3, ( $\text{pH}_{\text{PZC}}$  equal to 8.4), the IBP adsorption is promoted by dominant dispersive interactions as previously reported (Guedidi et al., 2013). The higher uptake of IBP at acidic pH with regard to neutrality is also probably related to the lower IBP solubility (of the molecular form) while the pH decreases, as its lower solubility promotes its adsorption on the carbon cloth (Shaw et al., 2005). The experimental IBP adsorption kinetics on C0 fabric were fitted to four models namely, the Lagergren pseudo-first-order model (1) (Lagergren, 1898), the pseudo-second-order model (2) (Ho and McKay, 1999), the Elovich model (3) (Chein and Clayton, 1980) and the intraparticle diffusion model (4) (Weber and Morris, 1963).

A pseudo first-order equation can be expressed as:

$$\frac{dq_t}{dt} = k_1(q_e - q_t) \quad (1)$$

where  $k_1$  is the rate constant of pseudo-first-order adsorption ( $\text{min}^{-1}$ ),  $q_e$  and  $q_t$  ( $\text{mg g}^{-1}$ ) are the amounts of adsorbed IBP at equilibrium and at time  $t$  (min) respectively.

The second-order equation is:

$$\frac{dq_t}{dt} = k_2(q_e - q_t)^2 \quad (2)$$

where  $k_2$  is the rate constant of pseudo-second-order adsorption ( $\text{g mg}^{-1} \text{min}^{-1}$ ),  $q_e$  and  $q_t$  ( $\text{mg g}^{-1}$ ) are the amounts of adsorbed IBP at equilibrium and at time  $t$  (min) respectively.

The Elovich equation is:

$$q_t = \frac{1}{\beta} \ln(\alpha \times \beta) + \frac{1}{\beta} \ln(t + t_0) \quad (3)$$

where  $\alpha$  is the adsorption initial rate ( $\text{mg g}^{-1} \text{min}^{-1}$ ,  $t_0 = 1/(\alpha \times \beta)$ ) and  $\beta$  is a constant ( $\text{g mg}^{-1}$ ) related to the external surface area and activation energy of adsorption (chemisorption).

The intraparticle diffusion model is formulated by:

$$q_t = k_p t^{0.5} \quad (4)$$

where  $k_p$  ( $\text{mg g}^{-1} \text{min}^{-1/2}$ ) is the intraparticle diffusion rate constant.

In order to estimate the best fit of the kinetic models to the experimental kinetic data, the optimization procedure requires different statistical parameters to be defined. In our study, the best fit model was evaluated by adjusted  $R^2$ , the Sum of the Square of the Errors (SSE), the Residual Root Mean Square Error (RMSE) and the chi-square test  $\chi^2$  expressed as follows:

$$\text{SSE} = \sum_{i=1}^n (q_{i(\text{exp})} - q_{i(\text{mod})})^2 \quad (5)$$

$$\text{RMSE} = \sqrt{\frac{1}{n} \left( \sum_{i=1}^n (q_{i(\text{exp})} - q_{i(\text{mod})})^2 \right)} \quad (6)$$

$$\chi^2 = \sum_{i=1}^n \frac{(q_{i(\text{exp})} - q_{i(\text{mod})})^2}{q_{i(\text{exp})}} \quad (7)$$

where  $q_{i(\text{exp})}$  is the adsorption capacity obtained from experiment,  $q_{i(\text{mod})}$  is the adsorption capacity obtained from kinetic model and  $n$  is the number of data points.

Table 5 shows the adsorption kinetic parameters calculated from the kinetic models. The profiles of each fitted curve at pH 3 and 7 are displayed in Fig. 6a and b respectively. The highest adjusted correlation coefficient  $R^2 = 0.99$  value obtained at pH 3 and lowest values of SSE (2810), RMSE (14.7) and  $\chi^2(8.90)$  for the Elovich model made it the best model for ibuprofen adsorption. It confirmed that the adsorption data were well represented by Elovich model (Table 5). The  $\alpha$  (Elovich parameter) adsorption initial rate of IBP was equal to  $3.929 \times 10^5 \text{ mg g}^{-1} \text{min}^{-1}$ .  $1/\beta$ , indicative of the number of sites available for adsorption, was equal to 23. Besides,  $1/\beta \times \ln(\alpha \beta)$  is the adsorption amount when  $\ln(t)$  is equal to zero. This value is helpful in understanding the adsorption behavior of the first step (Tseng, 2006); i.e., the IBP adsorption uptake by C0 when  $t = 1$  min is equal to 231.22  $\text{mg g}^{-1}$  which represents more than 50% of the total ibuprofen uptake.

**Table 5** Results of the best IBP kinetic fittings for C0 sample (pseudo-first order, pseudo-second order and Elovich models).

Kinetic model	Parameters	pH = 3	pH = 7
Pseudo-first-order	$q_e$ ( $\text{mg g}^{-1}$ )	383.3	168.4
	$k_1$ ( $\text{min}^{-1}$ )	0.110	0.003
	Adjusted- $R^2$	0.943	0.984
	SSE	$1.414 \times 10^4$	1182
	RMSE	32.98	8.59
	$\chi^2$	39.77	35.15
Pseudo-second-order	$q_e$ ( $\text{mg g}^{-1}$ )	395.6	183.7
	$k_2$ ( $\text{mg g}^{-1} \text{min}^{-1}$ )	$4.548 \times 10^4$	$2.63 \times 10^{-5}$
	Adjusted- $R^2$	0.974	0.994
	SSE	6443	442.50
	RMSE	22.26	5.26
	$\chi^2$	17.14	15.72
Elovich	$\alpha$ ( $\text{mg g}^{-1} \text{min}^{-1}$ )	$3.929 \times 10^5$	$1.5 \times 10^6$
	$\beta$ ( $\text{g mg}^{-1}$ )	0.042	0.163
	Adjusted- $R^2$	0.99	0.503
	SSE	2810	$3.79 \times 10^4$
	RMSE	14.7	48.7
	$\chi^2$	8.90	1716.72

Among all the tested kinetic models, the pseudo second order model was the best one for fitting IBP adsorption at pH 7 (it gives the best adjusted- $R^2 = 0.99$ , the lowest SSE = 442.5, RMSE = 5.26 and  $\chi^2 = 15.72$ ) (table 5). The intraparticle diffusion model proposed by Weber and Morris (1963) was not consistent with the experimental kinetics at pH 3 (Fig. 5a). However, at pH 7, the intraparticle diffusion model describes well the adsorption of IBP up to 600 min (intraparticle diffusion rate constant equal to  $5.764 \text{ mg g}^{-1} \cdot \text{min}^{-1/2}$ ). Fig. 6 shows the intraparticle diffusion plot of the adsorption of ibuprofen on the C0 cloth at 298 K, plot indicating three stages. The first stage represents the instantaneous adsorption or external surface adsorption up to 600 min, for which, the linear portion passes through the origin indicating that the rate of adsorption is controlled by the intraparticle diffusion. In the second stage, the regression is nearly linear but does not pass through the origin, suggesting that the intraparticle diffusion is not the only rate limiting mechanism in the adsorption process. The third region is the final equilibrium stage where the intraparticle diffusion starts to slow down due to the extremely low IBP concentrations remaining in the solutions. The  $Kp_i$  values which represent the rate parameter of  $i$  stage were found to be decreased ( $Kp_1 = 5.79$ ,  $Kp_2 = 1.98$ ,  $Kp_3 = 0.24$ ) indicating that the adsorption rate is initially faster and then slows down when the time is increased (Tan et al., 2009).

### 3.3. Adsorption isotherms

#### 3.3.1. Effect of temperature

Adsorption experiments were carried out at 298, 313 and 328 K. To investigate the temperature dependency of the

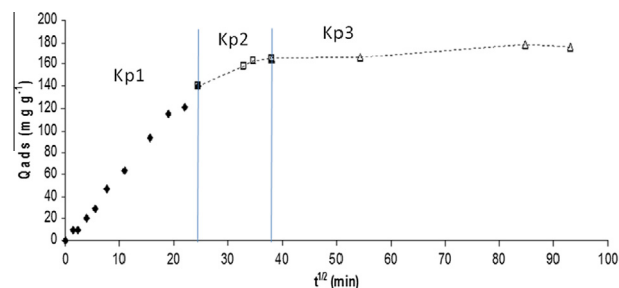


**Figure 6** Plot of intraparticle diffusion model for adsorption of IBP on C0 fabric at pH 7.

adsorption capacity, four equilibrium models were tested: Langmuir (Zhu et al., 2009), Freundlich, Langmuir–Freundlich (Yao, 2000) and Redlich–Peterson (Kumar and Porkodi, 2007). All the isotherms were simulated using an iterative procedure based on a non-linear least-squares algorithm.

The experimental data of IBP adsorption on C0 and modified activated carbon cloths at pH 3 were well fitted by the Langmuir–Freundlich model. In terms of adjusted- $R^2$ , the Langmuir–Freundlich model gives the best fitting (adjusted  $R^2 > 0.96$ ) in agreement with our previous work about the IBP adsorption on a granular activated carbon (Guedidi et al., 2013). Fig. 7 displays the Langmuir–Freundlich fits of isotherms at pH 3. With the rise of temperature the IBP maximum uptake increases for each cloth whatever the treatment which means that adsorption phenomenon is endothermic.

The adsorption equilibrium capacity of the activated carbon cloth C0 at 298 K was compared with the ones published recently of some other commercial and prepared activated

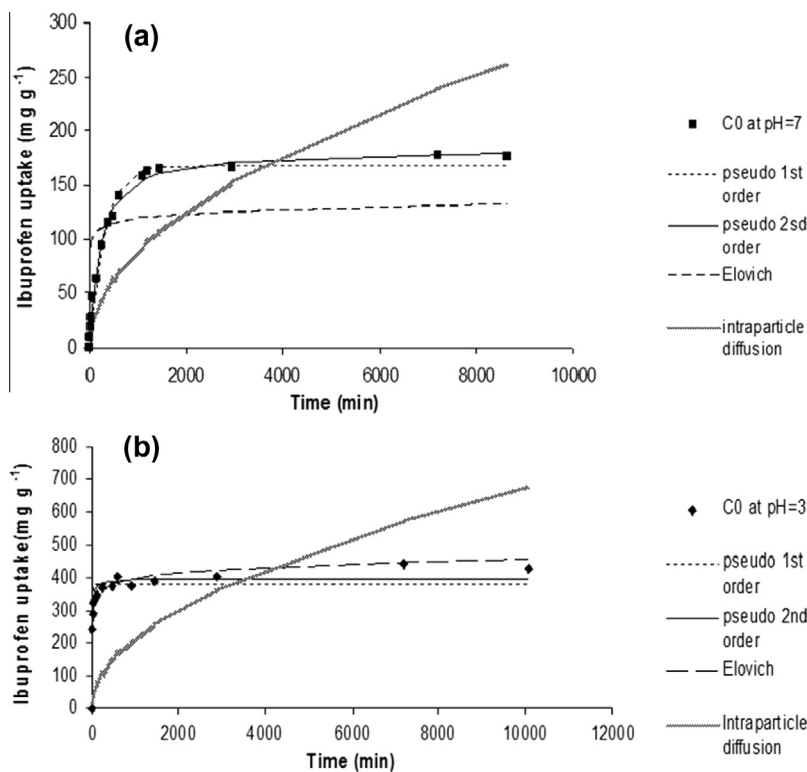


**Figure 5** Fitted profiles of ibuprofen adsorption kinetics of C0 sample at pH 3 (♦) (a) and at pH 7 (■) (b) by pseudo-first-order, pseudo-second order, Elovich and intraparticle diffusion models.



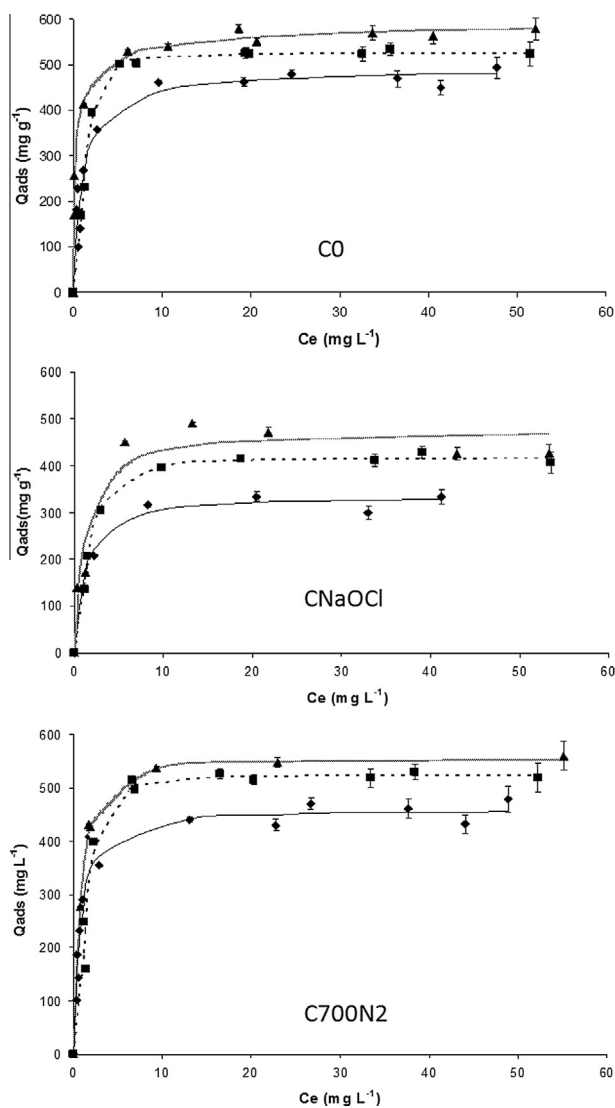


**Figure 7** Experimental IBP adsorption isotherms on CO, CNaOCl and C700N2 at pH 3 and at 298 K (◆), 313 K (▲) and 328 K (■) fitted by the Langmuir–Freundlich model (lines).

carbons (Table 6). We can notice that the adsorption capacity of the activated carbon cloth C0 toward ibuprofen is the highest and reaches about  $492 \text{ mg g}^{-1}$  at acidic pH. This value can

be correlated its highest surface area ( $S_{\text{BET}} \sim 1910 \text{ m}^2 \text{ g}^{-1}$ ) compared to the ones of the other sorbents ( $S_{\text{BET}} < 1160 \text{ m}^2 \text{ g}^{-1}$ ). However, the equilibrium time needed to reach this value is higher than for the granulated or powdered samples, which has to be correlated to a slower diffusion of the pollutant within the cloth fibers' porosity.

### 3.3.2. Thermodynamic parameters

The Langmuir–Freundlich simulations were used to calculate the thermodynamic parameters of adsorption. The Gibbs free energy change ( $\Delta G^\circ$ ), enthalpy change ( $\Delta H^\circ$ ) and entropy change ( $\Delta S^\circ$ ) were calculated according to the following thermodynamic equations:

$$\Delta G^\circ = -RT \ln K_d \quad (8)$$

where  $R$  ( $8.314 \text{ J mol}^{-1} \text{ K}^{-1}$ ) is the perfect gas constant,  $T$  is the solution temperature (K) and  $K_d$  is the distribution coefficient calculated as:

$$K_d = C_a/C_e \quad (9)$$

where  $C_a$  is the amount of IBP adsorbed at equilibrium ( $\text{mg L}^{-1}$ ),  $C_e$  is the concentration of IBP remaining in the solution at equilibrium ( $\text{mg L}^{-1}$ ).

$$\text{Thus, } \ln K_d = \Delta S^\circ / R - \Delta H^\circ / RT \quad (10)$$

The values of  $\ln K_d$  were plotted against  $1/T$ . The  $\Delta H^\circ$  and  $\Delta S^\circ$  values were calculated from the slope and intercept of the plot of Eq. (10). To compare the thermodynamic parameters of the three activated carbon cloths; they were calculated at constant adsorption uptake value equal to  $320 \text{ mg g}^{-1}$ .

The negative  $\Delta G^\circ$  values (Table 7), indicate the spontaneous nature and feasibility of the adsorption process of IBP on the different activated carbon cloths. Generally, the  $\Delta G^\circ$  value is in the range of 0 to  $-20 \text{ kJ mol}^{-1}$  and  $-80$  to  $-400 \text{ kJ mol}^{-1}$  for physical and chemical adsorptions, respectively (Yu et al., 2004). In this study, the  $\Delta G^\circ$  values are in the range of  $-1$  to  $-6.75 \text{ kJ mol}^{-1}$ , indicating that adsorptions are mainly physical. The highest  $\Delta G^\circ$  value for C700N2 indicates that the thermal treatment under  $\text{N}_2$  enhances the IBP adsorption. This can be related in one hand to the removing of oxygen groups from activated carbon surface after thermal treatment and in another hand to the creation of carbonyl groups that are responsible of the adsorption of ibuprofen through the donor acceptor phenomenon between ibuprofen and the carbonyl groups. The positive  $\Delta H^\circ$  values show that

**Table 6** Comparison of the performance toward the adsorption of ibuprofen on the C0 activated carbon cloth and other activated carbons reported in the literature.

Activated carbon (AC) origin	$S_{\text{BET}}$ ( $\text{m}^2 \text{ g}^{-1}$ )	Time for equilibrium	Adsorption capacity ( $\text{mg g}^{-1}$ )	References
AC cloth C0	1910	600 min (10 h)	491.9	This study
Commercial granular AC	800	4000 min (67 h)	138.1	Guedidi et al. (2013)
AC from artemisia vulgaris	358.2	> 5 h	16.73	Dubey et al. (2010)
AC obtained by chemical activation of cork powder	891	2 h	112.4	Mestre et al. (2009)
AC obtained by physical activation of cork powder	1060	2 h	106.4	Mestre et al. (2009)
AC obtained by physical activation of PET	1426	1 h	138.9	Mestre et al. (2009)
AC obtained by physical activation of coal	1156	0.5 h	131.6	Mestre et al. (2009)
AC obtained by physical activation of wood	899	0.2 h	131.6	Mestre et al. (2009)
AC obtained by physical activation of wood + boiling in 20% $\text{HNO}_3$	879	0.2 h	89.30	Mestre et al. (2009)
AC from olive waste cake	793	5 h	9.09	Baccar et al. (2012)
Commercial activated charcoal	–	~2 h	64.5	Khalaf et al. (2013)

**Table 7** Isothermic Gibbs free energy, enthalpy and entropy of adsorption of IBP (at constant adsorption uptake value  $Q_{\text{ads}} = 320 \text{ mg g}^{-1}$ ) at pH = 3.

Sample	C0	CNaOCl	C700N2
$\Delta G^\circ$ (kJ mol <sup>-1</sup> )	-5.8	-1.0	-6.7
$\Delta H^\circ$ (kJ mol <sup>-1</sup> )	45.0	60.2	11.6
$\Delta S^\circ$ (J K <sup>-1</sup> mol <sup>-1</sup> )	170.4	205.4	61.6

the adsorption process was endothermic in nature but less endothermal for C700N2.

The positive value of  $\Delta S^\circ$  shows a disorder increase at the solid liquid interface during the IBP adsorption. The high value of  $\Delta S^\circ$  for CNaOCl can be explained by the fact that NaOCl oxidation yields the surface more hydrophilic. As consequence, the oxygenated functional groups could interact with water molecules which need to be removed from the surface prior to IBP adsorption as previously suggested for adsorption of IBP on a granular activated carbon (Guedidi et al., 2013) and on a mesopore carbon (Dubey et al., 2010).

#### 4. Conclusion

The effect of NaOCl solution treatment or thermal treatment under nitrogen on a microporous activated carbon cloth surface chemistry and porosity were compared.

The adsorption kinetics of IBP on the raw carbon cloth were found to be accelerated by the decrease in pH. This is related to the decrease in the ibuprofen neutral form solubility and dominant dispersive interactions at pH lower than  $pK_a$  (4.7). The kinetics were well reproduced by the Elovich model at pH 3 and the pseudo second order at pH 7 on the whole time range. However, the best model particularly for time lower than 600 min was the intraparticle diffusion model. Such model suggests that the adsorption of ibuprofen in microporous cloth is controlled by the three molecular diffusion stages to the external surface, in the larger porous network, and finally in the ultramicropores. The CO<sub>2</sub> and N<sub>2</sub> adsorption analyses of raw and loaded IBP samples have shown that whatever the chemical treatment applied to the carbon cloth, the IBP adsorption might occur both in large ultramicropores and in supermicropores while the former pores might be totally blocked. The discrepancy between the measured and experimental uptake volumes has proved the incomplete filling of the accessible pore space attributed to the pore blockage by the ibuprofen molecule.

The IBP adsorption isotherms onto the raw and the modified activated carbon cloths were better fitted using Langmuir-Freundlich model at pH 3 in the temperature range 298–328 K. The adsorption of ibuprofen onto the activated carbon fabrics was found to be endothermic and the adsorption energy values indicated a physisorption process. The bleaching oxidation yielded to a slight micropore volume decrease and to the main formation of carboxylic, lactic and phenolic groups. The thermal treatment at 973 K under nitrogen flow did not change the porosity and micropore volume, removed initially the oxygen functional groups but gave rise after aging to the formation of carbonyl groups (ester and lactone) increasing the carbon basicity. This treatment promoted the IBP adsorption (at pH 3), yielding to a decrease in the adsorption Gibbs energy and enthalpy compared to pristine carbon cloth

possibly because of the advantage of a specific interaction of the carbonyl groups with the ibuprofen molecule. By contrast, the oxygenated surface formed through NaOCl impregnation resulted to a reduced ibuprofen adsorption capacity and an increase in the adsorption enthalpy.

#### Acknowledgment

Generous MIRA grant of the “Région Rhône-Alpes” (France) is thankfully acknowledged.

#### References

- Afkhami, A., Madrakian, T., Karimi, Z., Amini, A., 2007. Effect of treatment of carbon cloth with sodium hydroxide solution on its adsorption capacity for the adsorption of some cations. *Colloids Surf. A Physicochem. Eng. Aspects* 304, 36–40.
- Ania, C.O., Beguin, F., 2007. Mechanism of adsorption and electro-sorption of bentazone on activated carbon cloth in aqueous solutions. *Water Res.* 41, 3372–3380.
- Ayranci, E., Duman, O., 2006. Adsorption of aromatic organic acids onto high area activated carbon cloth in relation to wastewater purification. *J. Hazard. Mater.* B136, 542–552.
- Ayranci, E., Hoda, N., 2005. Adsorption kinetics and isotherms of pesticides onto activated carbon-cloth. *Chemosphere* 60, 1600–1607.
- Azaïs, T., Tourné-Péteilh, C., Aussenac, F., Baccile, N., Coelho, C., Devoisselle, J.-M., Babonneau, F., 2006. Solid-state NMR study of ibuprofen confined in MCM-41 material. *Chem. Mater.* 18, 6382–6390.
- Baccar, R., Sarrà, M., Bouzid, J., Feki, M., Blánquez, P., 2012. Removal of pharmaceutical compounds by activated carbon prepared from agricultural by-product. *Chem. Eng. J.* 211–212, 310–317.
- Biniak, S., Szymanski, G., Siedlewski, J., Swiatkowski, A., 1997. The characterization of activated carbons with oxygen and nitrogen surface groups. *Carbon* 35, 1799–1810.
- Boehm, H.P., 2002. Surface oxides on carbon and their analysis: a critical assessment. *Carbon* 40, 145–149.
- Cagnon, B., Py, X., Guillot, A., Joly, J.P., Berjoan, R., 2005. Pore modification of pitch-based activated carbon by NaOCl and air oxidation/pyrolysis cycles. *Microporous Mesoporous Mater.* 80, 183–193.
- Carrott, P.J.M., Nabais, J.M.V., Ribeiro Carrott, M.M.L., Menéndez, J.A., 2001. Thermal treatments of activated carbon fibres using a microwave furnace. *Microporous Mesoporous Mater.* 47, 243–252.
- Chein, S.H., Clayton, W.R., 1980. Application of Elovich equation to the kinetics of phosphate release and sorption in soils. *J. Soil Sci. Soc. Am.* 44, 265–268.
- Domingo-Garcia, M., Lopez-Garzon, F.J., Perez-Mendoza, M., 2000. Effect of some oxidation treatments on the textural characteristics and surface chemical nature of an activated carbon. *J. Colloid Interf. Sci.* 222, 233–240.
- Dubey, S.P., Dwivedi, A.D., Sillanpää, M., Gopal, K., 2010. Artemisia vulgaris-derived mesoporous honeycomb-shaped activated carbon for ibuprofen adsorption. *Chem. Eng. J.* 165, 537–544.
- Faur-Brasquet, C., Kadirvelu, K., Le Cloirec, P., 2002. Removal of metal ions from aqueous solution by adsorption onto activated carbon cloths: adsorption competition with organic matter. *Carbon* 40, 2387–2392.
- Franz, M., Arafat, H.A., Pinto, N.G., 2000. Effect of chemical surface heterogeneity on the adsorption mechanism of dissolved aromatics on activated carbon. *Carbon* 38, 1807–1819.
- Guedidi, H., Reinert, L., Lévêque, J.M., Soneda, Y., Bellakhal, N., Duclaux, L., 2013. The effect of the surface oxidation of activated carbon, the solution pH and the temperature on adsorption of ibuprofen. *Carbon* 54, 432–443.

- Ho, Y.S., McKay, G., 1999. Pseudo-second order model for sorption processes. *Process Biochem.* 34, 451–465.
- Jagiello, J., Olivier, J.P., 2009. A simple two-dimensional NLDFT model of gas adsorption in finite carbon pores. Application to pore structure analysis. *J. Phys. Chem. C.* 113, 19382–19385.
- Jagiello, J., Thommes, M., 2004. Comparison of DFT characterization methods based on N<sub>2</sub>, Ar, CO<sub>2</sub>, and H<sub>2</sub> adsorption applied to carbons with various pore size distributions. *Carbon* 42, 1227–1232.
- Jiang, B., Zheng, J., Lu, X., Liu, Q., Wu, M., Yan, Z., Qiu, S., Xue, Q., Wei, Z., Xiao, H., Liu, M., 2013. Degradation of organic dye by pulsed discharge non-thermal plasma technology assisted with modified activated carbon fibers. *Chem. Eng. J.* 215–216, 969–978.
- Kaneko, K., Ishii, C., 1992. Superhigh surface area determination of microporous solids. *Colloids Surf.* 67, 203–212.
- Khalaf, S., Al-Rimawi, F., Khamis, M., Zimmerman, D., Shuali, U., Nir, S., Scrano, L., Bufo, S.A., Karaman, R., 2013. Efficiency of advanced wastewater treatment plant system and laboratory-scale micelle-clay filtration for the removal of ibuprofen residues. *J. Environ. Sci. Health B* 48, 814–821.
- Kumar, K.V., Porkodi, K., 2007. Comments on “adsorption of 4-chlorophenol from aqueous solutions by xad-4 resin: isotherm, kinetic, and thermodynamic analysis”. *J. Hazard. Mater.* 143, 598–599.
- Lagergren, S., 1898. Zur theorie der sogenannten adsorption gel oster stoffe. *K. Sven. Vetenskapsakad. Handl.* 24, 1–39.
- Lerdkanchanaporn, S., Dollimore, D., 2000. The evaporation of Ibuprofen from Ibuprofen starch mixtures using simultaneous TG-DTA. *Thermochim. Acta* 357–358, 71–78.
- Lindqvist, N., Tuhkanen, T., Kronberg, L., 2005. Occurrence of acidic pharmaceuticals in raw and treated sewage and in receiving waters. *Water Res.* 39, 2219–2228.
- Menéndez, J.A., Phillips, J., Xia, B., Radovic, L.R., 1996. On the modification and characterization of chemical surface properties of activated carbon: in the search of carbons with stable basic properties. *Langmuir* 12, 4404–4410.
- Mestre, A.S., Bexiga, A.S., Proença, M., Andrade, M., Pinto, M.L., Matos, I., Fonseca, I.M., Carvalho, A.P., 2011. Activated carbons from sisal waste by chemical activation with K<sub>2</sub>CO<sub>3</sub>: kinetics of paracetamol and ibuprofen removal from aqueous solution. *Bioresour. Technol.* 102, 8253–8260.
- Mestre, A.S., Pires, J., Nogueira, J.M.F., Carvalho, A.P., 2007. Activated carbons for the adsorption of ibuprofen. *Carbon* 45, 1979–1988.
- Mestre, A.S., Pires, J., Nogueira, J.M.F., Parra, J.B., Carvalho, A.P., Ania, C.O., 2009. Waste-derived activated carbons for removal of ibuprofen from solution: role of surface chemistry and pore structure. *Bioresour. Technol.* 100, 1720–1726.
- Moreno-Castilla, C., Lopez-Ramon, M.V., Carrasco-Marin, F., 2000. Changes in surface chemistry of activated carbons by wet oxidation. *Carbon* 38, 1995–2001.
- Papirer, E., Li, S., Donnet, J.B., 1987. Contribution to the study of basic surface groups on carbon. *Carbon* 25, 243–247.
- Park, S.J., Park, B.J., Ryu, S.K., 1999. Electrochemical treatment on activated carbon fibers for increasing the amount and rate of Cr(VI) adsorption. *Carbon* 37, 1223–1226.
- Pereira, M.F.R., Soares, S.F., Orfao, J.J.M., Figueiredo, J.L., 2003. Adsorption of dyes on activated carbons: influence of surface chemical groups. *Carbon* 41, 811–821.
- Perrard, A., Retailleau, L., Berjoan, R., Joly, J.P., 2012. Liquid phase oxidation kinetics of an ex-cellulose activated carbon cloth by NaOCl. *Carbon* 50, 2226–2234.
- Pradhan, B.K., Sandle, N.K., 1999. Effect of different oxidizing agent treatments on the surface properties of activated carbons. *Carbon* 37, 1323–1332.
- Reffas, A., Bernardet, V., David, B., Reinert, L., BencheikhLehocine, M., Dubois, M., 2010. Carbons prepared from coffee grounds by H<sub>3</sub>PO<sub>4</sub> activation: characterization and adsorption of methylene blue and Nylosan Red N-2RBL. *J. Hazard. Mater.* 175, 779–788.
- Rong, H., Ryu, Z., Zheng, J., Zhang, Y., 2003. Influence of heat treatment of rayon-based activated carbon fibers on the adsorption of formaldehyde. *J. Colloid Interf. Sci.* 261, 207–212.
- Sabio, E., Gonzalez, E., Gonzalez, J.F., Gonzalez-Garcia, C.M., Ramiro, A., Ganan, J., 2004. Thermal regeneration of activated carbon saturated with p-nitrophenol. *Carbon* 42, 2285–2293.
- Shaw, L.R., Irwin, W.J., Grattan, T.J., Conway, B.R., 2005. The effect of selected water-soluble excipients on the dissolution of paracetamol and ibuprofen. *Drug Dev. Ind. Pharm.* 31, 515–525.
- Su, F., Lu, C., Hu, S., 2010. Adsorption of benzene, toluene, ethylbenzene and p-xylene by NaOCl-oxidized carbon nanotubes. *Colloids Surf. A Physicochem. Eng. Aspects* 353, 83–91.
- Swiatkowski, A., Deryo-Marczewska, A., Goworek, J., Bazewicz, S., 2004. Study of adsorption from binary liquid mixtures on thermally treated activated carbon. *Appl. Surf. Sci.* 236, 313–320.
- Tan, I.A.W., Ahmad, A.L., Hameed, B.H., 2009. Adsorption isotherms, kinetics, thermodynamics and desorption studies of 2,4,6-trichlorophenol on oil palm empty fruit bunch-based activated carbon. *J. Hazard. Mater.* 164, 473–482.
- Tseng, R.L., 2006. Mesopore control of high surface area NaOH-activated carbon. *J. Colloid Interf. Sci.* 303, 494–502.
- Valente Nabais, J.M., Carrott, P.J.M., Ribeiro Carrott, M.M.L., Menendez, J.A., 2004. Preparation and modification of activated carbon fibres by microwave heating. *Carbon* 42, 1315–1320.
- Verlicchi, P., Galletti, A., Petrovic, M., Barceló, D., 2010. Hospital effluents as a source of emerging pollutants: an overview of micropollutants and sustainable treatment options. *J. Hydrol.* 389, 416–428.
- Weber Jr., W.J., Morris, J.C., 1963. Kinetics of adsorption of carbon from solutions. *J. Sanit. Eng. Div. Am. Soc. Civ. Eng.* 89, 31–59.
- Xie, Y., Sherwood, P.M.A., 1990. X-ray photoelectron-spectroscopic studies of carbon fiber surfaces. 11. Differences in the surface chemistry and bulk structure of different carbon fibers based on poly(acrylonitrile) and pitch and comparison with various graphite samples. *Chem. Mater.* 2, 293–299.
- Yao, C., 2000. Extended and improved Langmuir equation for correlating adsorption equilibrium data. *Sep. Purif. Technol.* 19, 237–242.
- Yu, Y., Zhuang, Y.Y., Wang, Z.H., Qiu, M.Q., 2004. Adsorption of water-soluble dyes onto modified resin. *Chemosphere* 54, 425–430.
- Zhu, S., Yang, N., Zhang, D., 2009. Poly(N,N-dimethylaminoethyl methacrylate) modification of activated carbon for copper ions removal. *Mater. Chem. Phys.* 113, 784–789.